Supporting Information

Bimetallic $Ni_{2-x}Co_xP$ carbon nanofibers network: Solid-Solution-Alloy nano-architecture as efficient electrocatalysts for water splitting

Meijie Ding[a], Zhiqiang Wei[a,b*], Wenhua Zhao[b], Qiang Lu[c], Chenggong Lu[b], Meipan Zhou[a,b], Dexue Liu[a**], Hua Yang[a,b]

[a] *State Key Laboratory of Advanced Processing and Recycling of Non-ferrous Metals, Lanzhou University of technology, Lanzhou 730050, China*

[b] *School of Science, Lanzhou University of Technology, Lanzhou, 730050, China*

[c] *School of Materials Science and Engineering, Beihang University, Beijing, 100000, China*

∗ **Corresponding Author** e-mail: qianweizuo@163.com;

∗∗ **Corresponding Author** e-mail: dxliu@lut.edu.cn

1. Experimental Section

1.1. materials

All chemical reagents were used from commercial sources without further purification, and these materials include: Nickel nitrate hexahydrate ($Ni(NO_3)_2·6H_2O$, Aladdin), Cobalt nitrate hexahydrate ($Co(NO_3)_2·6H_2O$, Aladdin), Phosphorus red (P_4, Aladdin), absolute ethanol (C_2H_5OH, Aladdin) Potassium hydroxide (KOH, Aladdin), Polyvinylpyrrolidone ($(C_6H_9No)_n$, Aladdin), N, N-dimethylformamide (DMF, Aladdin), Ni foam ($1×2$ cm^2), Nafion solution (D-520 nafion solutions, Sigma-Aldrich) and ultrapure water (> 18 MΩ cm^{-1}).

1.2. Synthesis of sample

In this section, the synthesis of $Ni_{2-x}Co_xP$/CNFs precursor and $Ni_{2-x}Co_xP$/CNFs will be introduced in detail, and the synthesis process of the two materials can be seen in Scheme 1.

Typically, a varied amount of $Co(NO_3)·6H_2O$ and $Ni(NO_3)·6H_2O$ were dissolved into the mixed solvent consisting of 3 mL N, N-dimethylformamide, 1 mL deionized water, and 2 mL alcohol by stirring for 30 min to form a homogeneous solution, in which the offering molar ratio of metal cobalt to metal nickel was maintained at the level of 1:2, 1:1, 2:1, respectively, and further 1.8 g Polyvinylpyrrolidone was added into the forming homogeneous solution. After it was continuously stirred for 24 hours, the resulting mixture was transferred to an injection in an electrospinning device with aluminum foil as a nanofiber collector, and with the condition that the syringe speed was set to 0.25 mL h^{-1}, the distance between the aluminum foil and needle was 18 cm, and the positive high voltage to the electrospinning was 16.8 kV. The synthetic nanofiber membranes could be readily torn down from the aluminum foil, and the collected membranes were dried at 60 ℃ in a vacuum oven for 24 hours before the

subsequent chemical reactions. Afterwards, the dried products were first stabilized at 150 ℃ for 6 hours at speed of 1 ℃ min^{-1} in the tube furnace under Ar flow, and then heated to 350 ℃ at 1 °C min^{-1} and kept for 2 hours. Finally, the temperature zone was heated to 550 ℃ at 1 °C min^{-1} and maintained for 4 hours. When the reaction was cooled to room temperature, the $Ni_{2-x}Co_xP$/CNFs precursor sample was acquired in the alumina boat.

The $Ni_{2-x}Co_xP$/CNFs was obtained by a familiar vapor-phase phosphatization technology, in which 0.2 g of the sample and 1 g of red P were placed at two separate positions in a porcelain boat. Subsequently, the tube furnace was calcined at 650 °C for 2 hours with a heating rate of 1 °C min^{-1} in Ar atmosphere, and the loadings of $Ni_{2-x}Co_xP$/CNFs is about 1 g.

1.3. Physical measurements

The microstructure of the as-synthesized samples was determined by both the scanning electron microscope (SEM, JSM-6701F) and the transmission electron microscope (TEM, JEM 2100F), respectively. The products were determined by using an X-ray diffractometer (XRD, TK-XRD-201) with Cu Kα radiation in the 2θ range of from 10° to 90°. The surface element chemical state was characterized by X-ray photoelectron spectroscopy (XPS, Axis Ultra DLD). Raman measurements were obtained on a Raman microspectrometer (Horiba Jobin Yvon), with a laser wavelength of 633 nm. N_2 adsorption/desorption isotherms were performed at 7 K using a Surface Area Analyzer (JW-BK200B).

1.4. Electrochemical Measurements.

All electrochemical tests were recorded in 1 M KOH electrolyte using the CS310M electrochemical testing system. On a standard three-electrode configuration, Hg/HgO electrode and graphite rod were used as reference and counter electrodes, respectively. The third electrode can be fabricated by the following method: 4 mg of $Ni_{2-x}Co_xP$/CNFs and 40 uL of Nafion solution (5%) were dispersed in a 1 mL solvent mixture of water/ethanol (volume ratio = 7:3) simultaneously. The homogeneous ink was obtained after ultrasonication for 1 hour, and then the above 200 uL as-prepared ink, its mass loading of the sample being 0.8 mg cm^{-2}, was added dropwise on a Ni foam as the work electrode. All potentials reported in our manuscript were evaluated versus the reversible hydrogen electrode (RHE) by the formula of $E_{RHE} = E_{Hg/HgO} + (0.098 + 0.0591 \times pH)$ V. The polarization curves (2 mV s^{-1}) were recorded in 1 M KOH solution, the stability measurements were obtained by chronopotentiometry test for 24 hours, and the electrochemical impedance spectroscopy (EIS) was conducted from 10^{-2} to 10^6 Hz at a given potential (−0.106 V vs RHE). To evaluate the effective active electrode surface area, different scanning rates (20-200 mV s^{-1}) of cyclic voltammetry (CV) cycling were performed to calculate the double-layer capacitance (Cdl). All polarization curves are obtained by iR-corrections.

1.5. Computational methodology

All theoretical running program were obtained using first-principles, and carried out by the Vienna ab initio simulation package (VASP) program. The electron/ions exchange and correlation are described by using the functional of Perdew–Burke–Ernzerhof (PBE) with generalized gradient approximation (GGA) and the structures are relaxed using the conjugate gradient algorithm as implemented in VASP code until the forces and total energy on all atoms are converged to less than 0.01 eV $Å^{-1}$ and 1×10^{-5} eV. To optimize design model, the plane-wave cut-off energy is set at 500 eV and a 3 × 3 × 1 Monkhorst-Pack k-point sampling is used to obtained the Brillouin zone integration in this work. The final DFT model conform to the real structure of the real active.

The free energy is calculated by the following formula:

$$G=E+ZPE–TS \quad (1)$$

Where G is the free energy, E is the total energy from the DFT, ZPE is the zero point energy and TS is the entropy contribution (T values was 300 k).

The ZPE was obtained according to the following for mula:

$$ZPE = \sum hv \quad (2)$$

And the TS values are calculated after gaining the zero point energy according to the following formula:

$$TSv = kBT\ [\ \sum K \ln(1 - e\ 1 - hv/kBT\ ) + \sum K\ hv\ kBT\ 1\ (ehv/kBT - 1) + 1\ ] \quad (3)$$

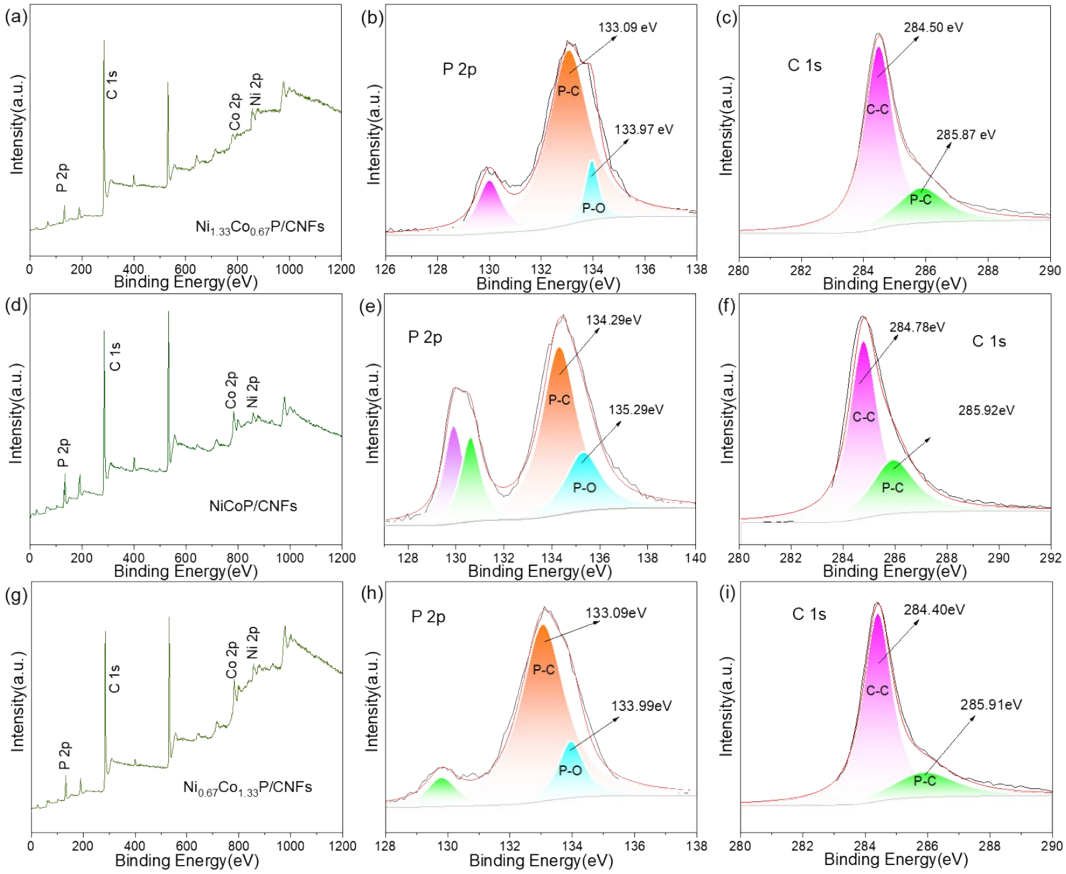

Figure S1. (a) XPS full spectrum of $Ni_{1.33}Co_{0.67}P$/CNFs. (b, c) High-resolution XPS spectra of P 2p and C 1s of $Ni_{1.33}Co_{0.67}P$/CNFs samples, respectively. (d) XPS full spectrum of $Ni_{1.33}Co_{0.67}P$/CNFs. (e, f) High-resolution XPS spectra of P 2p and C 1s of NiCoP/CNFs samples, respectively. (g) XPS full spectrum of $Ni_{0.67}Co_{1.33}P$/CNFs. (h, j) High-resolution XPS spectra of P 2p and C 1s of $Ni_{0.67}Co_{1.33}P$/CNFs samples, respectively.

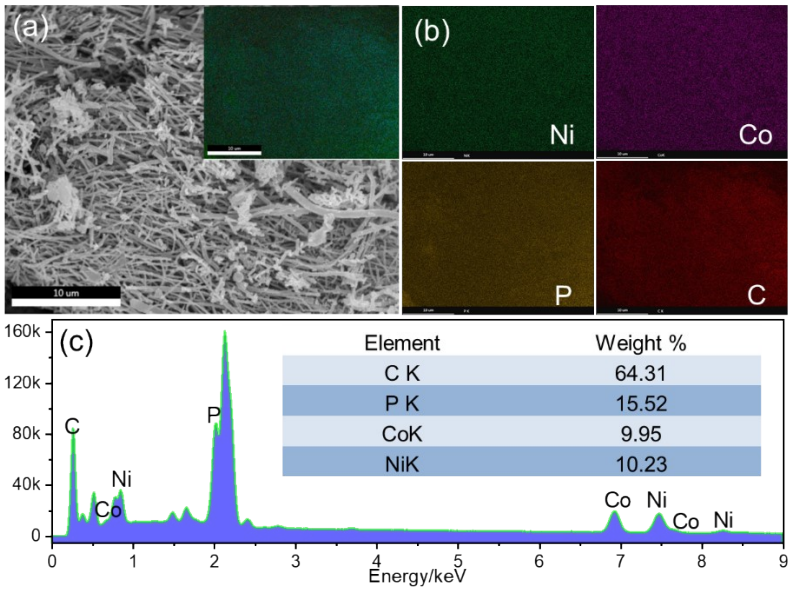

Figure S2. Morphology characterization of NiCoP/CNFs sample. (a) SEM images and (b) the corresponding element mapping of Ni, Co, P and C. (c) The EDX of NiCoP/CNFs sample.

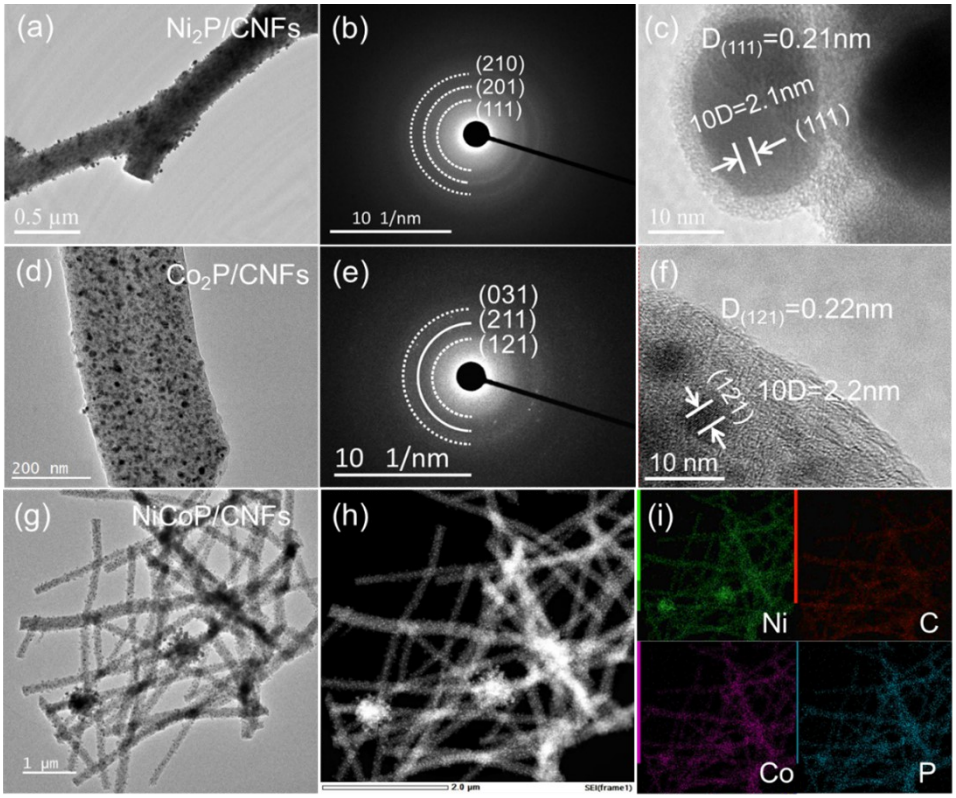

Figure S3. The TEM images, SAED pattern, and HRTEM images of (a-c) Ni_2P/CNFs, (d-f) Co_2P/CNFs, and the elemental mappings images of (g-i) NiCoP/CNFs sample.

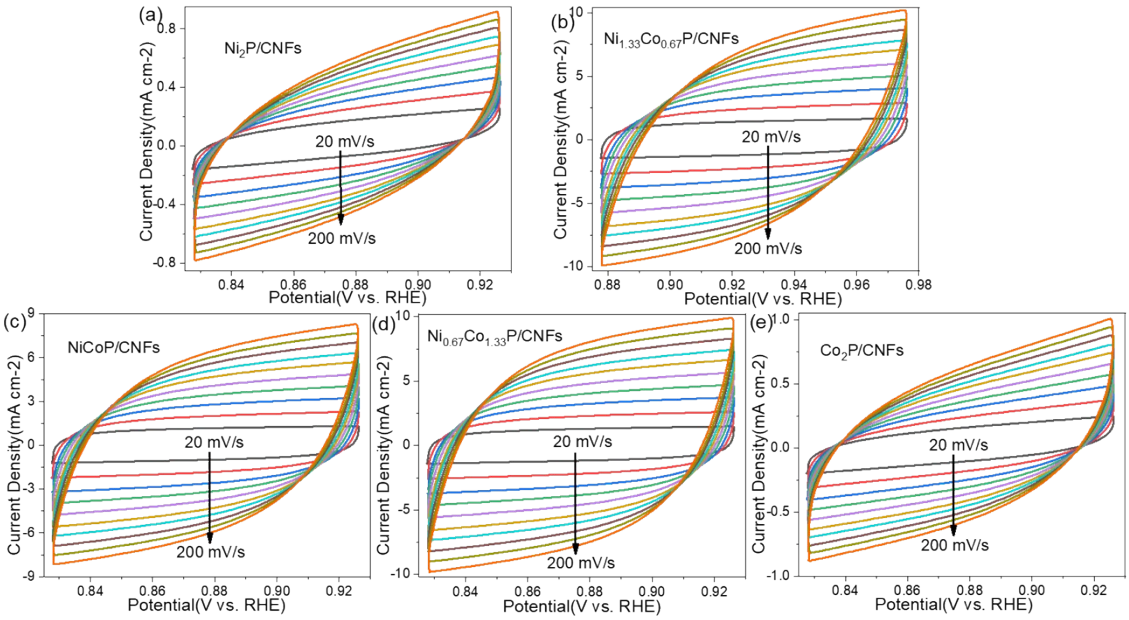

Figure S4. CV curves with different scan rates of the (a) Ni_2P/CNFs, (b) $Ni_{1.33}Co_{0.67}P$/CNFs (c) NiCoP/CNFs (d) $Ni_{0.67}Co_{1.33}P$/CNFs and (e) Co_2P/CNFs electrode for HER.

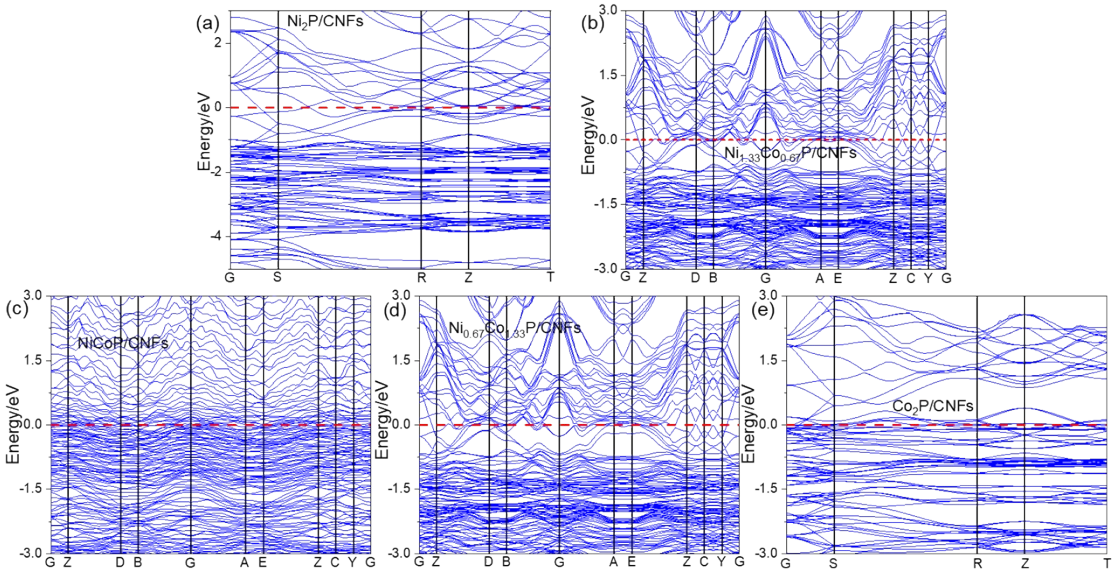

Figure S5. Energy-band structures of the (a) Ni_2P/CNFs, (b) $Ni_{1.33}Co_{0.67}P$/CNFs (c) NiCoP/CNFs (d) $Ni_{0.67}Co_{1.33}P$/CNFs and (e) Co_2P/CNFs materials.

Table S1 The HER performance of nanofiber electrocatalysts

Materials	Electrolyte	η10 [mV]	Tafel slope [mV dec^{-1}]	References
CoS_2-C@MoS_2 NFs	0.5 M H_2SO_4	173	61	[1]
$NiCo_2S_4$	0.5 M H_2SO_4	214	77.6	[2]
$NiCo_2S_4$/CNF	0.5 M H_2SO_4	266	114	[3]
FeCo/Co_2P@NPCF	1 M KOH	260	120	[4]
NiCoP/CNF700	1 M KOH	225	91	[5]
$NiCo_2Se_4$	0.5 H_2SO_4	168	49.8	[2]
Ni/Mo_2C-NCNFs	1 M KOH	143	57.8	[6]
Co/CoP@NC	1 M KOH	180	77.8	[7]
$Ni_{0.67}Co_{1.33}P$/CNFs	1 M KOH	118.76	78.2	This work

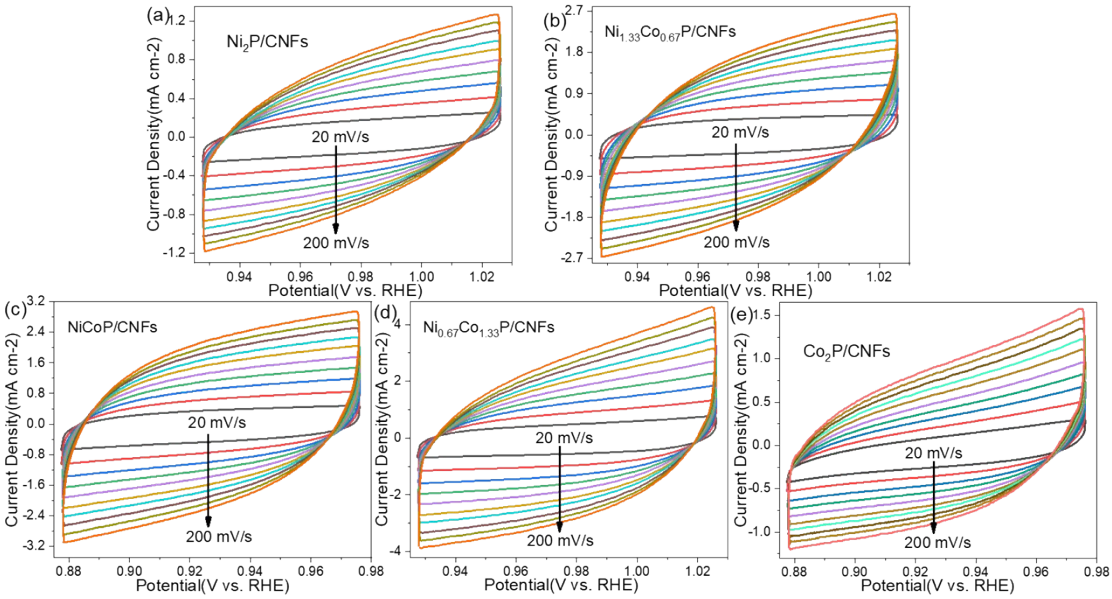

Figure S6. CV curves with different scan rates of the (a) Ni_2P/CNFs, (b) $Ni_{1.33}Co_{0.67}P$/CNFs (c) NiCoP/CNFs (d) $Ni_{0.67}Co_{1.33}P$/CNFs and (e) Co_2P/CNFs electrode for OER.

Table S2 The OER performance of nanofiber electrocatalysts

Materials	Electrolyte	η10 (mV)	Tafel slope (mV dec^{-1})	References
Co/N-CF	1 M KOH	380	92	[8]
CoNCNTF/CNFs	0.1 M KOH	380	66.8	[9]
Co/NCFs	1 M KOH	410	106.1	[10]
NiCo@N–C	0.1 M KOH	530	98	[11]
CoNi/BCF	0.1 M KOH	370	166	[12]
FeCo-NSCNF@NCNT	0.1 M KOH	360	49.5	[13]
CoNC-CNF-1000	0.1 M KOH	450	94	[14]
Co@N-CNFs	1 M KOH	436	105	[15]
$CuCo_2S_4$ NSs@N-CNFs	0.1 M KOH	315	48	[16]
$CoFe_2O_4$@NFs	1 M KOH	340	107	[17]
$Ni_{0.67}Co_{1.33}P$/CNFs	1 M KOH	271	52.9	This work

Table S3 The water splitting performance of nanofiber electrocatalysts

Materials	voltage	References
$Ni_{1.5}Co_{0.5}$@N-CNT/NFs	1.57V	[15]
FeCo@NC-12	1.71V	[18]
FeCo/Co_2P@NPCF	1.75V	[4]
Co-NiB@NF	1.72V	[19]
This work	1.53V	

References

1. Y. Zhu, L.F. Song, N. Song, M.X. Li, C. Wang, X.F. Lu, ACS Sustain Chem Eng. 7 (2019) 2899-2905.
2. W. Zong, R.Q. Lian, G.J. He, H.L. Guo, Y. Ouyang, J. Wang, F.L. Lai, Y. Miao, D.W. Rao, T.X. Liu, Electrochim Acta. 333 (2019) 135515.
3. J.C. Xu, J.Q. Rong, F.X. Qiu, Y.M. Zhu, K.F. Mao, Y.Y. Fang, D.Y. Yang, T. Zhang, ColloidInterface Sci. 555 (2019) 294.

4. Q. Shi, Q. Liu, Y. Ma, Z. Fang, Z. Liang, G. Shao, B. Tang, W.Y. Yang, L. Qin, X. Fang, Adv Energy Mater. 10 (2020) 1903854(1-11).
5. S. Surendran, S. Shanmugapriya, A. Sivanantham, S. Shanmugam, R.K. Selvan, Adv Energy Mater. 8 (2018) 1800553(1-18).
6. M. X. Li, Y. Zhu, H. Y. Wang, C. Wang, N. Pinna, X. F. Lu, Adv Energy Mater. 9 (2019) 1803185(1-11).
7. Y. Li, H.X. Li, K.Z. Cao, T. Jin, X.J. Wang, H.M. Sun, J.X. Ning, Y.J. Wang, L.F. Jiao, Energy Storage Mater. 12 (2018) 44-53.
8. P.P. Sun, D. Zhang, M. He, Z. Zuo, N. Huang, X. Lv, Y.H. Sun, X.H. Sun, Electrochim Acta. 337 (2020) 135848.
9. D.X. Ji, L. Fan, L.L. Li, N. Mao, X.H. Qin, S.J. Peng, S. Ramakrishna, Carbon. 142 (2018) 379-387.
10. H.Z. Li, M.Q. An, Y.W. Zhao, S. Pi, C.J. Li, W. Sun, H.G. Wang, Appl Surf Sci. 478 (2019) 560-566.
11. Y. Fu, H.Y. Yu, C. Jiang, T.H. Zhang, R. Zhan, X.W. Li, J. F. Li, J.H. Tian, R.Z. Yang, Adv Funct Mater. 28 (2018) 129-138.
12. W.J. Wan, X.J. Liu, H.Y. Li, X.Y. Peng, D.S. Xi, J. Luo, Appl Catal B. 240 (2019) 193-200.
13. K. Fu, Y. Wang, L.C. Mao, X.X. Yang, W. Peng, J.H. Jin, S.L. Yang, G. Li, J Power Sourc. 421 (2019) 68-75.
14. W.M. Zhang, X.Y. Yao, S.N. Zhou, X.W. Li, L. Li, Z. Yu, L. Gu, Small. 14 (2018) 1800423(1-8).
15. T.F. Li, S.L. Li, Q.Y. Liu, J.W. Yin, D.M. Sun, M.Y. Zhang, L. Xu, Y.W. Tang, Y.W. Zhang, Adv Sci. 7 (2019) 1902371(1-9).
16. Z.H. Pan, H. Chen, J. Yang, Y.Y. Ma, Q.C. Zhang, Z.K. Kou, X.Y. Ding, Y.J. Pang, L. Zhang, Q.L. Gu, C.L. Yan, J. Wang, Adv Sci. 6 (2019) 1900628(1-10).
17. Z.M. Zhang, J.Y. Zhang, T. Wang, Z.W. Li, G.J. Yang, H.Q. Bian, J.Y. Li, D.Q. Gao, RSC Adv. 8 (2018) 5338-5343.
18. F. Aftab, H. Duran, K. Kirchhoff, M. Zaheer, B. Iqbal, M. Saleem, S.N. Arshad, Chem Cat Chem. 12 (2019) 932-943.
19. Z.Y. Wu, W.B. Ji, B.C. Hu, H.W. Liang, X.X. Xu, Z.L. Yu, B.Y. Li, S.H. Yu, Nano Energy. 51 (2018) 286-293.